Orientational configurations of the C_{60} molecules in the (2×2) superlattice on a solid C_{60} (111) surface at low temperature

Haiqian Wang, Changgan Zeng, Bing Wang, and J. G. Hou*
Structure Research Laboratory, University of Science and Technology of China, Hefei, Anhui 230026, People's Republic of China

Qunxiang Li and Jinlong Yang
Open Laboratory of Bond Selective Chemistry, University of Science and Technology of China, Hefei, Anhui 230026, People's Republic of China

(Received 17 July 2000; published 7 February 2001)

The orientational configurations of C_{60} molecules on the surface of a multilayer C_{60} island with a (111)-terminating plane were studied at 78 K by using a scanning tunneling microscope. A 2×2 superlattice, which resulted from the orientational ordering of the C_{60} molecules, was observed. In each unit cell of the superlattice, one C_{60} molecule with a three-lobe intramolecular pattern, and three C_{60} molecules with dumbbell-like intramolecular patterns, were clearly resolved. In combination with the theoretical analysis and simulation, the orientational configurations of the C_{60} molecules were determined.

DOI: 10.1103/PhysRevB.63.085417 PACS number(s): 61.48.+c. 68.65.−k, 73.61.Wp

I. INTRODUCTION

A C_{60} molecule is composed of 12 pentagons and 20 hexagons. This elegant cage structure includes the C_{60} solid with many interesting physical and chemical properties. In addition to the translational ordering in the traditional solids, there is also molecular orientational ordering in a C_{60} solid. Understanding the orientational ordering is a basic issue for studying fullerene-based materials.

At room temperature a bulk C_{60} crystal adopts a fcc structure (space group $Fm\bar{3}m$).[1–4] Molecules which are orientationally disordered rotate nearly freely and independently of each other.

In the temperature range of 90–260 K, the molecules in solid C_{60} lose two of their three degrees of rotational freedom, and the lattice structure is transformed into a simple cubic (sc, space group $Pa\bar{3}$), known as the rotational ordered phase.[3–6] From a physical standpoint, the lowering of the crystal symmetry is caused by the assignment of a local threefold axis to each of the four distinct molecules in a unit cell. In this low-temperature ordered phase, there are two energetically, nearly degenerated, orientational variants for each molecule, corresponding to counterclockwise rotation from a standard orientation through $\sim22°$ and $\sim82°$, respectively, about a local threefold cubic [111], $[1\bar{1}\bar{1}]$, $[\bar{1},\bar{1},1]$, or $[\bar{1},1,\bar{1}]$ direction. The energy difference between these two orientational variants is ~11 meV, and the energetic barrier between them is 235–280 meV.[3,4] In an idealized ordered structure (corresponding to a setting angle of $\sim22°$), the relative orientation of adjacent molecules is stabilized by aligning a bond common to two hexagons (hereafter denoted as a 6:6 bond) on one molecule opposite the pentagonal face of an adjacent C_{60} molecule. Another structure (called the ''defect structure''), which corresponds to a setting angle of $\sim82°$, places the 6:6 bond of one C_{60} molecule opposite a hexagonal face of an adjacent C_{60} molecule. David *et al.*[5] described the low-temperature rotational ordered phase by a uniaxial reorientation, which takes the form of a fast 60° hop with relatively long residence times at sites corresponding to setting angles of about $(22+60n)°$ $(n=0,1,2,\ldots)$.

Below 90 K, the C_{60} molecules are frozen into a glassy phase (or rotational frozen phase). In this state, the rotational freedoms of the molecules are totally lost; each molecule randomly occupies one of the two orientation-dependent local-energy minima. It was suggested that in this temperature range the orientation of the majority of C_{60} molecules is described by a setting angle of $\sim22°$, while the minority finds itself in an orientation with a setting angle of about 82°.[5]

In analogy to the orientational fcc-sc transition in the bulk, on the surface of C_{60} films with two or more layers of C_{60} molecules, a 1×1 to 2×2 disorder-order transition with $T_c=225$–235 K (about 30 K lower than that of the bulk fcc-sc transition) was confirmed by electron-energy-loss spectroscopy (EELS), low-energy election-diffraction (LEED), and helium-atom scattering diffraction (HAS) studies, as well as by theoretical calculations.[7–11]

However, the EELS, LEED, and HAS techniques can only provide statistical information on the surface superlattice, rather than give the orientational configurations of the molecules. The scanning tunneling microscopy (STM) technique has the advantage of imaging a solid surface in real space with atomic resolution; this makes it a powerful tool for studying the orientational configurations of C_{60} molecules grown on solid surfaces.[12–14]

In this paper, we focus our attention on the orientational configurations of C_{60} molecules on the (111)-terminating plane of a multilayer C_{60} film. In order to reduce the influences of the substrate, and thus to study the intrinsic properties of the orientational ordering, we grow a multilayer film with C_{60} islands of up to about 10 ML thick. A 2×2 superlattice, which resulted from the orientational ordering of the C_{60} molecules, was observed on the surface of a multilayer C_{60} islands by STM at 78 K. In combination with theoretical simulation, the orientational configurations of C_{60} molecules in the 2×2 superlattice are determined. To our knowledge,

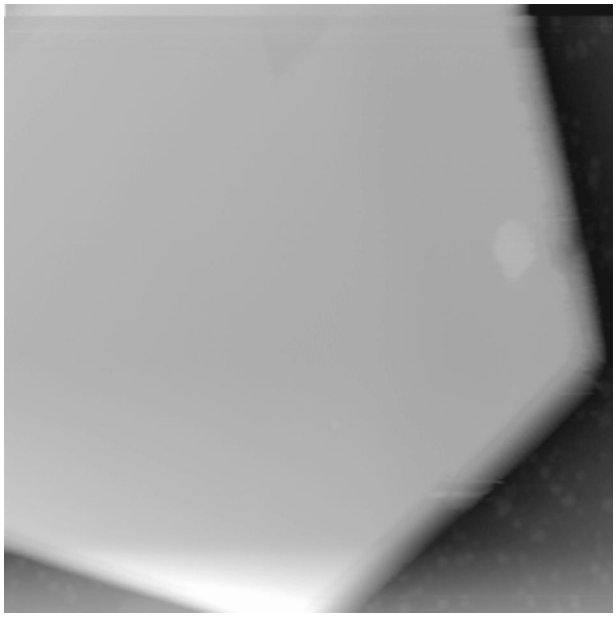

FIG. 1. A 300×300-nm^2 STM topography image of a 10-ML C_{60} island grown on a Si(100) 2×1 surface.

this is the first example of a 2×2 superlattice observed directly by STM on the C_{60}(111) surface.

II. EXPERIMENT

The experiments were carried out at a base pressure below 1×10^{-11} mbar by using an OMICRON low-temperature STM with an electrochemically etched tungsten tip, which was subjected to a careful cleaning treatment. A Si(100)-(2×1) surface, with a low defect density was obtained by the standard outgas and flash-annealing procedures.[15] C_{60} molecules were sublimed from a Knudsen cell to a nominal thickness of 2 ML on the Si(100)-(2×1) substrate, which was kept at room temperature. The as-deposited C_{60} film was then subjected to a post annealing to a temperature of about 300 °C. This annealing process induced the C_{60} molecules to crystallize into multilayer islands. Figure 1 shows a C_{60} island with about 10 ML of close-packed C_{60} molecules.

The STM images were recorded at 78 K. Since the C_{60} film is a semiconductor with a bank gap of about 1.6–1.9 eV,[16–18] it is crucial to set a high bias voltage and to keep a small tunneling current during scanning. In this experiment, the sample bias voltage was set to 5.5 V and the tunneling current was typically kept at 50 pA.

III. RESULTS AND DISCUSSIONS

Figure 2(a) shows an empty-state topography STM image which was taken at 78 K on the island surface, as shown in Fig. 1. C_{60} molecules crystallize into multilayer islands with a close-packed molecular arrangement, which corresponds to the (111) plane in the bulk fcc structure. Instead of the orientational glassy phase as predicted in the bulk,[5] in the experimental scope an ordered 2×2 superlattice was observed

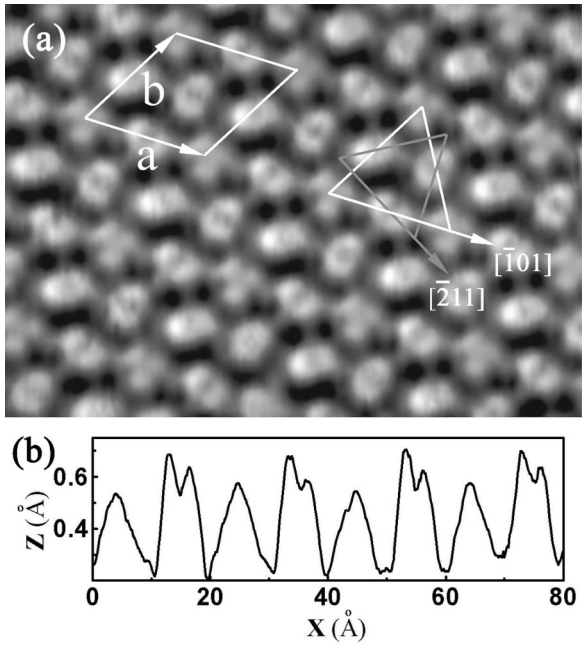

FIG. 2. (a) Empty-state topography STM image on a C_{60} island surface. A 2×2 superlattice can be clearly resolved. (b) The line profile along the direction of the base vector **a** indicates that the heights of C_{60} molecules with three-lobe intramolecular patterns are lower than those of the dumbbell-like ones.

on the surface of the island. In each unit cell of the superlattice, one C_{60} molecule with a three-lobe intramolecular pattern and three C_{60} molecules with dumbbell-like intramolecular patterns were clearly resolved. The line profiles of the STM image also clearly demonstrate a 2×2 superlattice of the surface. For example, Fig. 2(b) displays a line profile along the direction of the base vector **a** of the unit cell, as indicated in Fig. 2(a), in which the lower peaks correspond to the three-lobe C_{60} molecules and the higher double peaks correspond to the dumbbell-like ones. Statistical results over the highest parts of the molecules indicate that, on average, the height of the C_{60} molecules with three-lobe intramolecular patters are about 0.1 Å lower than the dumbbell-like ones.

At room temperature, we did not observe any intramolecular patterns of the C_{60} molecules. This indicates that all the molecules rotate freely at room temperature, which is consistent with previous results.[7–10] We also cooled the sample down to liquid-nitrogen temperature, and warmed it up to room temperature several times, and obtained the same STM images. This indicates that our result is reproducible.

It is believed that different intramolecular patterns result from different orientations of the C_{60} molecules.[13,14] The three-lobe features of the C_{60} intramolecular image indicate that the corresponding molecules stopped their rotation and existed on the surface with a hexagon facing up. As for the three dumbbell-like intramolecular patterns in a unit cell, they vary their orientations about the [111] direction (normal to the sample surface) by different angles. The triangles in Fig. 2(a) illustrate the orientational relations of the three dumbbell-like C_{60} molecules (gray triangle) with respect to the three-lobe ones (white triangle). There are three three-

lobe C_{60} molecules at the corners of the white triangle, and three dumbbell-like ones in the middle of each side. The three sides of the white triangle lie in the $[10\bar{1}]$, $[\bar{1}10]$, and $[0\bar{1}1]$ directions, respectively. The gray triangle is obtained by drawing lines through the centers of the three dumbbell-like C_{60} molecules along the $[1\bar{2}1]$, $[\bar{2}11]$, and $[11\bar{2}]$ directions, respectively. It can be seen that the three dumbbell-like patterns of the C_{60} molecules lie approximately in the directions of the three sides of the gray triangle, which rotates by 30° clockwise with respect to the sides of the white triangle.

In general, however, the observed intramolecular patterns are not directly related to the atomic structure of the molecules, but to the electronic structure of the fullerenes on the surfaces. In order to correlate the STM image [Fig. 2(a)] to the orientational configurations of the C_{60} molecules, we conducted a theoretical simulation of the C_{60} molecules with different orientations.

The C_{60} island is about 10 ML thick. For such a multilayer film, the influence of the substrate to the C_{60} molecules on the surface should be negligible, so only the interactions from the neighboring C_{60} molecules are important in determining the orientations of the C_{60} molecules. However, the interactions between C_{60} molecules are of van der Waals type. Even though this interaction is important in determining the orientational ordering of the molecules at low temperature, it does not influence the local density of states (LDOS) of the C_{60} molecules significantly. Thus, in the simulation, as an approximation, we only simulate the LDOS of a free C_{60} molecule with different orientations.

We adopted Tersoff and Hamann's formula[19,20] and its extension to simulate STM images. In this method, the tunneling current in the STM can be expressed as

$$I(V) \propto \int_{E_F}^{E_F+eV} dE \rho(\mathbf{r},E), \tag{1}$$

$$\rho(\mathbf{r},E) = \sum_i |\psi_i(\mathbf{r})|^2 \delta(E-E_i), \tag{2}$$

where $\rho(\mathbf{r},E)$, $\psi_i(\mathbf{r})$, and E_F are the LDOS of the C_{60} molecule, the wave function with energy E_i, and the Fermi energy, respectively. Equations (1) and (2) assume a constant density of states of the tip which allows us to obtain STM images from only the LDOS of the sample surface. This assumption is tenable when the separation between the tip and sample is large enough. The experimental conditions for obtaining Fig. 2(a) meet this requirement. It is known that the LDOS near the E_F makes a dominant contribution to the STM images. Hence we can obtain the LDOS by adding up several molecular orbitals with the same weight.

The electronic structures of the free C_{60} molecules were calculated by using a discrete-variational–local-density approximation method which was described in detail elsewhere.[21,22] In the formulation of Kohn-Sham equations we used an exchange and correlation potential of the von Barth–Hedin[23] form, with parameters taken from Moruzzi *et al.*[24] The atomic basis functions, representing the electron orbitals, were $1s^{2.0}2s^{2.0}2p^{2.0}$. Using 600 sample points per atom in the numerical integration, we achieved sufficient convergence (less than 10^{-5}e) for the self-consistent charge process. Finally, the LDOS distribution on the upper hemisphere with a 16 bohr radius ($R_{t\text{-}s}$) from the center of C_{60} was calculated.

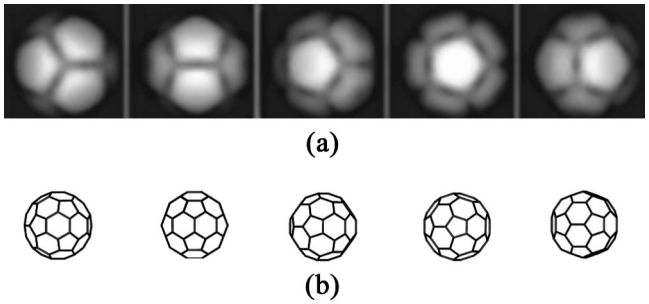

FIG. 3. (a) Simulated empty-state STM images of a free C_{60} molecule with five kinds of high-symmetry rotational orientations corresponding to (b) schematic diagrams of C_{60} with a hexagon, a 6:6 bond, a 5:6 bond, a pentagon, and an atop atom facing up, respectively, from left to right.

Figure 3 displays the theoretically simulated constant current empty-state STM images of a free C_{60} with five kinds of high-symmetry orientations. Comparing Figs. 3(a) and 3(b), we can see that the bright spots correspond to the pentagonal rings. This can be explained with the excess LDOS in the empty-state level at pentagonal rings which consist of five sp^2 bonds. Among these simulated images, threefold and twofold symmetry intramolecular patterns can be observed, respectively, in C_{60} molecules with a hexagon and a 6:6 bond facing up.

As mentioned above, in the idealized ordered structure inside a C_{60} solid, the relative orientation of adjacent molecules is stabilized by aligning an electron-rich 6:6 bond on one molecule opposite an electron-poor pentagonal face of an adjacent C_{60} molecule.[6] The high symmetry of the C_{60} molecule allows these interactions to be optimized identically for all 12 nearest neighbors. On the surface of a C_{60} solid, the driving force for the three-dimensional fcc-sc transition is absent due to the breaking of translational symmetry. For example, molecules at the surface have only nine neighbors instead of 12 in the bulk. However, the existence of the 2×2 superlattice indicates that a crystal field involving nine nearest neighbors of C_{60} molecules is still capable of driving the molecules to an orientationally ordered state.[11]

In analogy to the idealized ordered structure in the bulk (corresponding to a setting angle of $\sim 22°$), we suppose a schematic diagram for the orientational configurations of C_{60} molecules on the (111) surface, as shown in Fig. 4(a). Figure 4(b) is obtained by choosing simulated empty-state STM images of the free C_{60} molecules with a hexagon and a 6:6 bond facing up (Fig. 3), and arranging them according to the orientational configurations as illustrated in Fig. 4(a). Figure 4(c) is an enlarged STM image of Fig. 2(a). For purposes of comparison we shade out some of the molecules here. From Fig. 4, we can see that the theoretical simulation reproduces the main features of the STM image. In each unit cell of the superlattice, one C_{60} molecule with a three-lobe intramolecular pattern and three C_{60} molecules with dumbbell-like in-

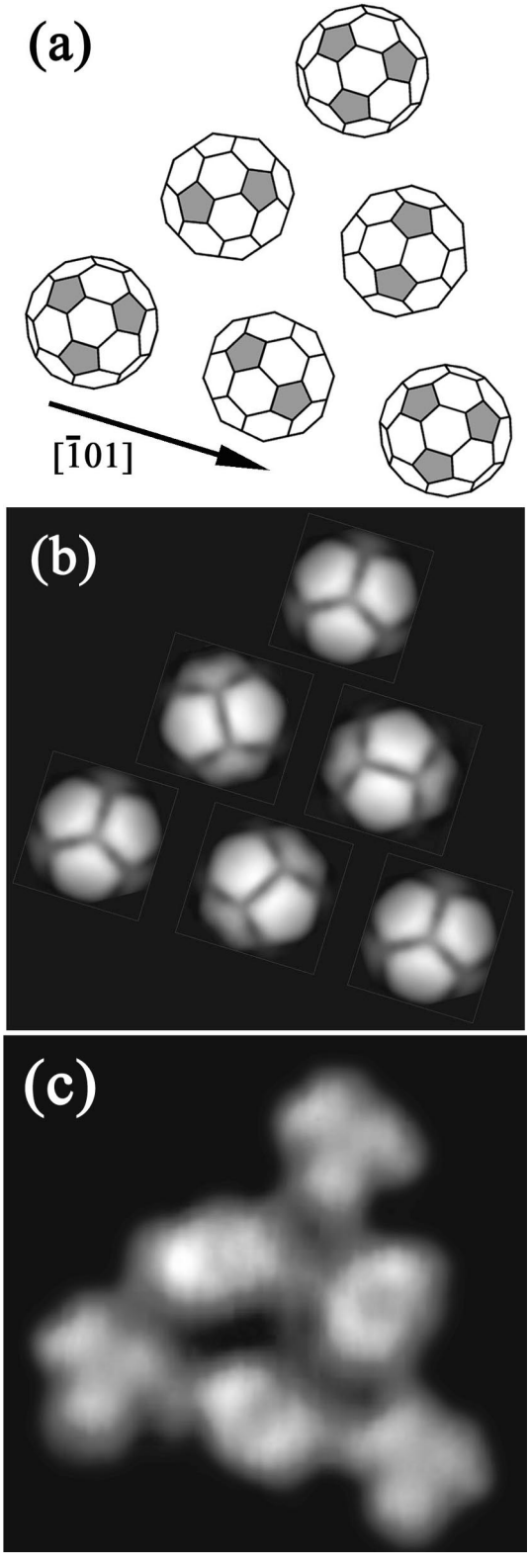

FIG. 4. (a) Schematic diagram of the C_{60} orientational configurations on the $C_{60}(111)$ surface. The shaded pentagons are the electronic rich regions corresponding to the bright spots in the STM images, (b) the simulated empty-state STM image, and (c) an enlarged image of Fig. 2(a) with some of the molecules shaded out.

tramolecular patterns are revealed. Moreover, the orientations of the intramolecular patterns also coincide with those shown in Fig. 2(a). For example, in Fig. 4(b), the three threefold symmetry C_{60} molecules form a triangle corresponding to the white triangle in Fig. 2(a), and the three twofold C_{60} molecules form a triangle corresponding to the gray triangle in Fig. 2(a).

By setting the simulated LDOS to a constant value, we can obtain the contour of a C_{60} molecule. In this way, we can also scale the heights of C_{60} molecules with different orientations theoretically. For example, when we set the cutoff of the LDOS to 1×10^{-7} bohr^{-3}, the heights of C_{60} molecules with hexagon and 6:6 bonds facing up are 7.84 and 7.93 Å, respectively. Considering that such calculated heights are dependent on the cutoff of the LDOS and, on the other hand, that the measured heights may be influenced by possible relaxations of the surface molecules, we cannot compare them directly. However, qualitatively, these calculated heights can explain the phenomenon that the three-lobe C_{60} molecules are lower than the dumbbell ones (Fig. 2). Therefore, this result also supports the orientational configurations illustrated in Fig. 4(a). Based on the above results and discussions, we conclude that the orientational configurations of the C_{60} molecules on a (111) surface are similar to those in a bulk material.

Inside a crystalline C_{60} solid, because of the high-symmetry crystal field, the orientational configurations of all the C_{60} molecules can be determined with a single order parameter.[5,6] On a C_{60} solid surface, the breaking of translational lattice symmetry makes the C_{60} molecules remain in an asymmetric crystal field. This makes the C_{60} molecules in the four sublattices inequivalent. In a previous theoretical work, by taking account of two order parameters, Passerone and Tosatti[11] predicted that there are two kinds of sublattices in a unit cell. However, by careful examination of the results in Fig. 2, we can see that the three dumbbell-like C_{60} molecules in a 2×2 unit cell are not exactly identical, and some dumbbell-like patterns may appear brighter on one side than on the other side. This can be explained as the molecules tilt from the 6:6 bond orientation slightly to the atop orientation, which can be understood by consulting Fig. 3. This result indicates that two order parameters may be not enough for optimizing the orientational configurations of the C_{60} molecules on the surface. Savin *et al.*[4] computed the interaction energies for a pair of C_{60} molecules; their results indicate that the 6:6 bond to pentagon configuration is not the lowest in energy. This implies that once the symmetry of the C_{60} array is changed, the orientational configurations of the C_{60} molecules will very likely change. In the present case, on the $C_{60}(111)$ surface, the nearest-neighbor molecules are changed from 12 (in the bulk) to 9. Thus we think that the breaking symmetry on the surface will very likely result in the orientations of the C_{60} molecules becoming optimized again.

In order to obtain a full understanding of the orientational configurations of C_{60} molecules on the surface, further detailed theoretical studies are still to be explored. These include optimizing the orientational configurations energetically, and simulating the LDOS's of the C_{60} molecules by

considering interactions of the neighboring molecules. Our STM observations on the surface of solid C_{60} provide good initial orientational settings for this future work.

IV. SUMMARY

In summary, instead of the orientational glassy phase as predicted in the bulk, an ordered 2×2 superlattice was observed on the (111) surface of a multilayer C_{60} film by STM at 78 K. In each unit cell of the superlattice, one C_{60} molecule with a three-lobe intramolecular pattern and three C_{60} molecules with dumbbell-like intramolecular patterns were clearly resolved. By comparing the intramolecular patterns of a STM image with the theoretical simulated results, we found that orientational configurations of the C_{60} molecules on the surface are similar to those in the bulk, except for some complex details. This similarity indicates that it is the interaction of the neighboring C_{60} molecules that drives the molecules to an orientational ordered state.

ACKNOWLEDGMENTS

This work was supported by the NSF, the ICQS of Chinese Academy of Sciences, and the NKBRSF of China under the Grant No. G1999075305.

*Author to whom the correspondence should be addressed.

[1] P.A. Heiney, J.E. Fischer, A.R. Mc Ghie, W.J. Romanov, J.P. McCauley, Jr., and A.B. Smith III, Phys. Rev. Lett. **66**, 2911 (1991).
[2] P.A. Heiney, J. Phys. Chem. Solids **53**, 1333 (1992).
[3] M. S. Dresselhaus, G. Dresselhaus, and P. C. Eklund, in *Science of Fullerenes and Carbon Nanotubes* (Academic Press, San Diego, 1996), pp. 171–196, and references therein.
[4] S. Savin, A.B. Harris, and T. Yildirim, Phys. Rev. B **55**, 14 182 (1997).
[5] W.I.F. David, R.M. Ibberson, T.J.S. Dennis, J.P. Hare, and K. Prassides, Europhys. Lett. **18**, 219 (1992).
[6] W.I.F. David, R.M. Ibberson, J.C. Matthewman, K. Prassides, T.J.S. Dennis, J.P. Hare, H.W. Kroto, R. Taylor, and D.R.M. Walton, Nature (London) **353**, 147 (1991).
[7] Z.Y. Li, Surf. Sci. **441**, 366 (1999).
[8] A. Goldoni, C. Cepek, and S. Modesti, Phys. Rev. B **54**, 2890 (1996).
[9] P.J. Benning, F. Stepniak, and J.H. Weaver, Phys. Rev. B **48**, 9086 (1993).
[10] A. Glebov, V. Senz, J.P. Toennies, and G. Gensterblum, J. Appl. Phys. **82**, 2329 (1997).
[11] D. Passerone and E. Tosatti, Surf. Rev. Lett. **4**, 859 (1997).
[12] T. Sakurai, X.D. Wang, Q.K. Xue, Y. Hasegawa, T. Hashizume, and H. Shinohara, Prog. Surf. Sci. **51**, 263 (1996).
[13] X. Yao, R.K. Workman, C.A. Peterson, D. Chen, and D. Sarid, Appl. Phys. A: Mater. Sci. Process. **66**, S107 (1998).
[14] J.G. Hou, Yang Jinlong, Wang Haiqian, Li Qunxiang, Zeng Changgan, Lin Hai, D.M. Chen, and Zhu Qingshi, Phys. Rev. Lett. **83**, 3001 (1999).
[15] R.M. Tromp, R.J. Hamers, and J.E. Demuth, Phys. Rev. Lett. **55**, 1303 (1985).
[16] O. Janzen and W. Mönch, J. Phys.: Condens. Matter **11**, L111 (1999).
[17] S. Saito and A. Oshiyama, Phys. Rev. Lett. **66**, 2637 (1991).
[18] J. Guo, D.E. Ellis, and D.J. Lam, Chem. Phys. Lett. **176**, 203 (1991).
[19] J. Tersoff and D.R. Hamann, Phys. Rev. Lett. **50**, 1998 (1983).
[20] J. Tersoff and D.R. Hamann, Phys. Rev. B **31**, 805 (1985).
[21] B. Delley and D.E. Ellis, J. Chem. Phys. **76**, 1949 (1982).
[22] B. Delley, D.E. Ellis, A.J. Freeman, E.J. Baerends, and D. Post, Phys. Rev. B **27**, 2132 (1983).
[23] U. von Barth and L. Hedin, J. Phys. C **5**, 1629 (1972).
[24] V.L. Moruzzi, J.F. Janak, and A.R. Williams, *Calculated Electronic Properties of Metals* (Pergamon, New York, 1978).